

Optical Magnus effect on gravitational lensing

Yusuke Nishida

Department of Physics, Institute of Science Tokyo, Ookayama, Meguro, Tokyo 152-8551, Japan

(Dated: March 2026)

The optical Magnus effect refers to transverse shift of a trajectory of light caused by its polarization and appears as a correction to geometrical optics at the linear order in wavelength. Here, we start from Maxwell's equations in a curved spacetime to derive the equation of motion for a wave packet of circularly polarized light, which confirms the known result involving the helicity-dependent anomalous velocity with some generalization and clarification. We then study possible consequences of the optical Magnus effect on gravitational lensing in the Schwarzschild spacetime as well as under a weak gravitational potential in an expanding spacetime. Among others, by formulating the lens equation modified to incorporate the optical Magnus effect, the Einstein ring is found impossible to emerge from a point source for any axially symmetric thin lens. Analytic solutions to the modified lens equation are also obtained for simple lens models, illuminating how image formation is affected by the optical Magnus effect.

I. INTRODUCTION

Polarization has been an important probe in high-precision astrophysics and cosmology, providing us with new insights unavailable from intensity measurements alone. Among others, the B -mode polarization of the cosmic microwave background is useful to constrain models of cosmic inflation and primordial gravitational waves because it cannot be produced by density fluctuations [1–4]. The polarization images taken by the Event Horizon Telescope and the Imaging X-ray Polarimetry Explorer already brought out information on structures and dynamics of magnetized plasmas around supermassive black holes [5–7]. Furthermore, possible polarization modes of gravitational waves are expected to serve as diagnostics to test alternative theories of gravity [8–10]. The polarization of light is typically considered to be transported simply from a source to an observer, with its trajectory following a null geodesic of background spacetime independent of the wavelength and polarization of light. This is an assumption relying on the geometrical-optics approximation valid in the limit of negligible wavelength [11, 12].

However, the trajectory of light is to acquire dependence on its polarization by incorporating the wave nature of light at the linear order in wavelength. This phenomenon in classical optics is known as the optical Magnus effect or the spin Hall effect of light [13–19]. It manifests itself as transverse shift of a trajectory of circularly polarized light when it propagates through an inhomogeneous optical medium. Because a spacetime under a static gravitational potential can be modeled as an optical medium with a spatially varying refractive index [20], a gravitational analog of the optical Magnus effect is expected and has indeed been derived with various approaches such as the Foldy-Wouthuysen transformation [21, 22], the Wentzel-Kramers-Brillouin approximation [23, 24], the path integral formulation [25, 26], and the Mathisson-Papapetrou-Dixon equations [27, 28]. See also Refs. [29–32] for recent developments as well as Refs. [33, 34] for reviews on this subject.

The purpose of our work is to study possible consequences of the optical Magnus effect on gravitational lensing, which is the deflection of light by a massive object predicted by Einstein's theory of general relativity [11, 12]. In order to make our work self-contained, we first derive the equation of motion for a wave packet of circularly polarized light starting from Maxwell's equations in a curved spacetime in Sec. II. We then apply the resulting equation of motion to the gravitational lensing in the Schwarzschild spacetime in Sec. III as well as under a weak gravitational potential in an expanding spacetime in Sec. IV. Finally, our findings are summarized in Sec. V together with some outlook. We set the speed of light to $c = 1$ in Sec. II and Appendices, whereas c is presented explicitly in the other sections.

II. OPTICAL MAGNUS EFFECT

A. Maxwell's equations

In order to derive the gravitational analog of the optical Magnus effect, we start from Maxwell's equations in a curved spacetime,

$$\nabla_a F^{ab} = 0, \quad \nabla_a \tilde{F}^{ab} = 0, \quad (1)$$

where F^{ab} is the electromagnetic tensor and $\tilde{F}^{ab} = -\epsilon^{abcd} F_{cd}/2$ is its dual with $\epsilon^{0123} = -1/\sqrt{-g}$. The metric in the foliated spacetime is decomposed as

$$ds^2 = -\alpha^2 dt^2 + \gamma_{ij}(dx^i + \beta^i dt)(dx^j + \beta^j dt) \quad (2)$$

in terms of the lapse function α , shift vector β^i , and spatial metric γ_{ij} on the spacelike hypersurface Σ_t . The timelike unit vector normal to Σ_t reads $n^a = (1/\alpha, -\beta^i/\alpha)$ and thus $n_a = (-\alpha, 0, 0, 0)$. The electric and magnetic fields measured by an Eulerian observer are then provided by

$$E^a = F^{ab} n_b, \quad B^a = \tilde{F}^{ab} n_b. \quad (3)$$

Because of $n_a E^a = n_a B^a = 0$, the electromagnetic tensor and its dual can be expressed as

$$F^{ab} = n^a E^b - n^b E^a + \epsilon^{abc} B_c, \quad (4)$$

$$\tilde{F}^{ab} = n^a B^b - n^b B^a - \epsilon^{abc} E_c, \quad (5)$$

with $\epsilon^{abc} \equiv n_d \epsilon^{dabc}$.

Maxwell's equations in Eq. (1) are projected along n_a by $n_b \nabla_a F^{ab} = 0$, leading to

$$D_i E^i = 0, \quad D_i B^i = 0, \quad (6)$$

where D_i is the covariant derivative compatible with γ_{ij} . On the other hand, they are projected onto Σ_t by $(\delta^i_b + n^i n_b) \nabla_a F^{ab} = 0$, leading to

$$\partial_t E^i = (\mathcal{L}_\beta + \alpha K) E^i + \epsilon^{ijk} D_j (\alpha B_k), \quad (7)$$

$$\partial_t B^i = (\mathcal{L}_\beta + \alpha K) B^i - \epsilon^{ijk} D_j (\alpha E_k), \quad (8)$$

where $\mathcal{L}_\beta E^i = \beta^j D_j E^i - E^j D_j \beta^i$ is the Lie derivative along the shift vector and $K = -\nabla_a n^a$ is the trace of extrinsic curvature tensor. See Refs. [35–37] for further details. Obviously, Eqs. (6), (7), and (8) represent Gauss's law, Ampère's law, and Faraday's law in a curved spacetime, respectively.

We now assume an irrotational spacetime with $\beta^i = 0$ and introduce a densitized complex field as $\Psi^i \equiv \sqrt{\gamma} (E^i + iB^i) / \sqrt{2}$. By employing $\alpha K = -\partial_t \ln \sqrt{\gamma} + D_j \beta^j$ and the Levi-Civita symbol $\epsilon^{ijk} = \sqrt{\gamma} \epsilon^{ijk} \in \{0, \pm 1\}$, each pair of equations for electric and magnetic fields can be combined into

$$\partial_i \Psi^i = 0, \quad (9)$$

$$\partial_t \Psi^i = -i \epsilon^{ijk} \partial_j \left(\frac{\alpha}{\sqrt{\gamma}} \Psi_k \right). \quad (10)$$

The second equation leads to the continuity equation,

$$\partial_t \rho + \partial_i j^i = \partial_t \left(\frac{\alpha}{\sqrt{\gamma}} \gamma_{ij} \right) \Psi^{*i} \Psi^j, \quad (11)$$

where Ψ^{*i} is the complex conjugate of Ψ^i and

$$\rho = \frac{\alpha}{\sqrt{\gamma}} \gamma_{ij} \Psi^{*i} \Psi^j, \quad j^i = -i \epsilon^{ijk} \frac{\alpha^2}{\gamma} \Psi_j^* \Psi_k \quad (12)$$

are proportional to the energy density and the Poynting vector, respectively. Therefore, the total energy of electromagnetic field is conserved only when $\alpha \gamma_{ij} / \sqrt{\gamma}$ is independent of time. For example, it is achieved for $\alpha = a(t) \sqrt{A(\mathbf{x})}$ and $\gamma_{ij} = a(t)^2 C(\mathbf{x}) \delta_{ij}$, which is the case considered in the following discussion.

B. Wave packet motion

Maxwell's equations under

$$ds^2 = a(t)^2 [-A(\mathbf{x}) dt^2 + C(\mathbf{x}) \delta_{ij} dx^i dx^j] \quad (13)$$

are thus brought into the Dirac-like equation,

$$\partial_i \Psi^i(t, \mathbf{x}) = 0, \quad (14)$$

$$i \partial_t \Psi^i(t, \mathbf{x}) = \epsilon^{ijk} \partial_j [v(\mathbf{x}) \Psi^k(t, \mathbf{x})]. \quad (15)$$

Here, $a(t)$ is the scale factor, t is the conformal time, \mathbf{x} are the comoving coordinates, $v(\mathbf{x}) \equiv \sqrt{A(\mathbf{x})/C(\mathbf{x})}$ is an effective velocity, and the summation over repeated indices is taken regardless of their positions.

We then introduce the Fourier representation of complex electromagnetic field,

$$\Psi(t, \mathbf{x}) = \int \frac{d\mathbf{k}}{(2\pi)^3} \psi(t, \mathbf{k}) \mathbf{e}(\mathbf{k}) e^{\lambda i \mathbf{k} \cdot \mathbf{x}}, \quad (16)$$

where $\mathbf{e}(\mathbf{k}) \equiv [\hat{\mathbf{e}}_1(\mathbf{k}) + i \hat{\mathbf{e}}_2(\mathbf{k})] / \sqrt{2}$ is a complex polarization vector defined in terms of three mutually orthogonal unit vectors $\hat{\mathbf{k}}, \hat{\mathbf{e}}_1(\mathbf{k}), \hat{\mathbf{e}}_2(\mathbf{k})$ satisfying $\hat{\mathbf{k}} = \hat{\mathbf{e}}_1(\mathbf{k}) \times \hat{\mathbf{e}}_2(\mathbf{k})$. Gauss's law in Eq. (14) is ensured by $\mathbf{k} \cdot \mathbf{e}(\mathbf{k}) = 0$, whereas $\lambda = \pm 1$ specifies the helicity corresponding to right-handed and left-handed circular polarizations. The latter can be understood because Eq. (15) for constant v is solved by $\psi(t, \mathbf{k}) \sim e^{-\lambda i v |\mathbf{k}| t}$, so that the electric field evolves as $\mathbf{E}(t, \mathbf{x}) \sim \cos(v |\mathbf{k}| t - \mathbf{k} \cdot \mathbf{x}) \hat{\mathbf{e}}_1(\mathbf{k}) + \lambda \sin(v |\mathbf{k}| t - \mathbf{k} \cdot \mathbf{x}) \hat{\mathbf{e}}_2(\mathbf{k})$ for a given wavevector.

Because of the energy conservation, the complex electromagnetic field can be normalized as

$$\int d\mathbf{x} v(\mathbf{x}) |\Psi(t, \mathbf{x})|^2 = 1, \quad (17)$$

where the integrand represents an energy density normalized by the total energy. We now assume that the electromagnetic field forms a wave packet localized in both position and wavevector spaces. Namely, $|\Psi(t, \mathbf{x})|^2$ is localized at $\mathbf{x} \approx \bar{\mathbf{x}}(t)$ and $|\psi(t, \mathbf{k})|^2$ at $\mathbf{k} \approx \bar{\mathbf{k}}(t)$, where $\bar{\mathbf{x}}(t)$ and $\bar{\mathbf{k}}(t)$ are a mean position and a mean wavevector of the wave packet at a given time, respectively. This assumption allows us to make the approximations of

$$x^i |\Psi(t, \mathbf{x})|^2 \approx \bar{x}^i(t) |\Psi(t, \mathbf{x})|^2, \quad (18)$$

$$k_i |\psi(t, \mathbf{k})|^2 \approx \bar{k}_i(t) |\psi(t, \mathbf{k})|^2. \quad (19)$$

For example, the mean position under the above normalization is provided by

$$\bar{x}^i(t) \approx \int d\mathbf{x} v(\mathbf{x}) x^i |\Psi(t, \mathbf{x})|^2. \quad (20)$$

By employing the Fourier representation in Eq. (16) together with $x^i e^{\lambda i \mathbf{k} \cdot \mathbf{x}} = -\lambda i \partial_{k_i} e^{\lambda i \mathbf{k} \cdot \mathbf{x}}$ and $\psi(t, \mathbf{k}) \equiv e^{-\lambda i \varphi(t, \mathbf{k})} |\psi(t, \mathbf{k})|$, we obtain

$$\bar{x}^i(t) \approx [\partial_{k_i} \varphi(t, \mathbf{k}) - \mathcal{A}^i(\mathbf{k})]_{\mathbf{k} \rightarrow \bar{\mathbf{k}}(t)}, \quad (21)$$

where $\mathcal{A}^i(\mathbf{k}) = -\lambda i \mathbf{e}^*(\mathbf{k}) \cdot \partial_{k_i} \mathbf{e}(\mathbf{k})$ is the so-called Berry connection.

Ampère's and Faraday's law in Eq. (15) is obtained by the principle of least action from

$$S = \int dt d\mathbf{x} \left[v(\mathbf{x}) \Psi^{*i}(t, \mathbf{x}) i \overleftrightarrow{\partial}_t \Psi^i(t, \mathbf{x}) - \varepsilon^{ijk} [v(\mathbf{x}) \Psi^{*i}(t, \mathbf{x}) \overleftrightarrow{\partial}_j [v(\mathbf{x}) \Psi^k(t, \mathbf{x})]] \right], \quad (22)$$

with $\Psi^* \overleftrightarrow{\partial} \Psi \equiv [\Psi^* (\partial \Psi) - (\partial \Psi^*) \Psi] / 2$. The equation of motion for the wave packet is then derived by regarding the action for the complex electromagnetic field as that for the wave packet [38, 39]. The Fourier representation in Eq. (16) substituted into the above action leads to

$$S \approx \lambda \int dt [\partial_t \varphi(t, \mathbf{k}) - v(\mathbf{x}) |\mathbf{k}|]_{\mathbf{x} \rightarrow \bar{\mathbf{x}}(t), \mathbf{k} \rightarrow \bar{\mathbf{k}}(t)}. \quad (23)$$

The first term can be expressed as $\partial_t \varphi(t, \bar{\mathbf{k}}(t)) \approx \dot{\varphi}(t, \bar{\mathbf{k}}(t)) - \dot{\bar{k}}_i(t) [\bar{x}^i(t) + \mathcal{A}^i(\bar{\mathbf{k}}(t))]$ in terms of the total time derivative and the mean position in Eq. (21). Therefore, the action reads $S \approx \lambda \int dt L$ with the Lagrangian provided by

$$L = \bar{k}_i(t) \dot{\bar{x}}^i(t) - v(\bar{\mathbf{x}}(t)) |\bar{\mathbf{k}}(t)| - \dot{\bar{k}}_i(t) \mathcal{A}^i(\bar{\mathbf{k}}(t)). \quad (24)$$

Finally, the Euler-Lagrange equation with respect to $\bar{x}^i(t)$ leads to

$$\dot{\bar{k}}_i(t) = -|\bar{\mathbf{k}}(t)| \partial_i v(\bar{\mathbf{x}}(t)), \quad (25)$$

whereas that with respect to $\bar{k}_i(t)$ leads to

$$\begin{aligned} \dot{\bar{x}}^i(t) &= v(\bar{\mathbf{x}}(t)) \partial_{k_i} |\bar{\mathbf{k}}(t)| + \varepsilon^{ijk} \dot{\bar{k}}_j(t) \mathcal{B}_k(\bar{\mathbf{k}}(t)) \\ &= v(\bar{\mathbf{x}}(t)) \frac{\bar{k}_i(t)}{|\bar{\mathbf{k}}(t)|} - \lambda \varepsilon^{ijk} \partial_j v(\bar{\mathbf{x}}(t)) \frac{\bar{k}_k(t)}{|\bar{\mathbf{k}}(t)|^2}, \end{aligned} \quad (26)$$

where $\mathcal{B}(\mathbf{k}) \equiv \partial_{\mathbf{k}} \times \mathcal{A}(\mathbf{k}) = \lambda \mathbf{k} / |\mathbf{k}|^3$ is the so-called Berry curvature. The resulting two equations constitute the equation of motion for the wave packet of circularly polarized light. It is valid as long as a variation of potential is negligible over a spatial extension of wave packet, requiring $|\partial \ln v(\bar{\mathbf{x}}(t))| \ll |\bar{\mathbf{k}}(t)|$. The first term of Eq. (26) together with Eq. (25) is equivalent to the null geodesic of background spacetime in Eq. (13) as shown in Appendix A. On the other hand, the second term of Eq. (26) transverse to both potential gradient and wavevector is known as the anomalous velocity, providing a correction to geometrical optics at the linear order in wavelength. Because its sign is opposite for right-handed and left-handed circular polarizations, the trajectory of light is to acquire dependence on its polarization, which is nothing other than the gravitational analog of the optical Magnus effect.

We note that although the consistent expression can be found in Refs. [21, 22, 25, 26], our alternative derivation allows an expanding spacetime as well as a strong gravitational potential described within Eq. (13). It also clarifies that the optical Magnus effect is a purely classical phenomenon with no quantum mechanics at all. In

particular, \hbar never appears unless it is introduced artificially as a bookkeeping parameter to perform the systematic expansion over wavelength. Furthermore, the same equation motion is expected for a wave packet of circularly polarized gravitational wave by regarding $\lambda \rightarrow \pm 2$ as its helicity [24, 26, 31]. A heuristic derivation with our approach applied to linearized Einstein's equations is presented in Appendix B. In the following sections, we simplify the notation as $\bar{x}^i(t) \rightarrow x^i$, $\bar{k}_i(t) \rightarrow k_i$, $|\bar{\mathbf{k}}(t)| \rightarrow k$, and $v(\bar{\mathbf{x}}(t)) \rightarrow v$.

III. SCHWARZSCHILD SPACETIME

We first apply the resulting equation of motion to the gravitational lensing in the Schwarzschild spacetime with particular attention to its photon sphere and black hole shadow. The metric in isotropic coordinates is provided by

$$ds^2 = -\left(\frac{1 - \frac{r_s}{4r}}{1 + \frac{r_s}{4r}}\right)^2 (cdt)^2 + \left(1 + \frac{r_s}{4r}\right)^4 \delta_{ij} dx^i dx^j, \quad (27)$$

where $r_s = 2GM/c^2$ is the Schwarzschild radius and $r = \sqrt{x^2 + y^2 + z^2} > r_s/4$. Then, the equation of motion is brought into

$$\frac{dk_i}{dt} = -k \frac{x^i}{r} \partial_r v, \quad (28a)$$

$$\frac{dx^i}{dt} = v \frac{k_i}{k} - \lambda \varepsilon^{ijk} \frac{x^j k_k}{r k^2} \partial_r v, \quad (28b)$$

with $v = c [1 - r_s/(4r)] / [1 + r_s/(4r)]^3$.

A. Photon sphere

The photon sphere consists of unstable circular orbits of light around a massive object [11]. Because

$$\frac{dr}{dt} = v \frac{x^i k_i}{rk}, \quad \frac{dk}{dt} = -\frac{x^i k_i}{r} \partial_r v, \quad (29a)$$

$$\frac{d(x^i k_i)}{dt} = (v - r \partial_r v) k \quad (29b)$$

are obtained from the above equation of motion, constant r is possible only when $v = r \partial_r v$. It is achieved outside the event horizon at

$$r = \frac{2 + \sqrt{3}}{4} r_s, \quad (30)$$

corresponding to $R = r [1 + r_s/(4r)]^2 = 3r_s/2$ in the Schwarzschild coordinates. This is the radius of photon sphere, which is found unaffected by the optical Magnus effect.

When r is constant, k is also constant because of $x^i k_i = 0$. Then, Eq. (28) under $v = r \partial_r v$ leads to

$$\frac{d^2 x^i}{dt^2} = -\left(\frac{v}{r}\right)^2 \left(1 + \frac{\lambda^2}{r^2 k^2}\right) x^i, \quad (31)$$

so that the orbit is provided by $x^i(t) = \cos(\omega t)x^i(0) + \sin(\omega t)\dot{x}^i(0)/\omega$ with

$$\omega = \frac{v}{r} \sqrt{1 + \frac{\lambda^2}{r^2 k^2}}. \quad (32)$$

This is the frequency of circular motion of light, which is found to acquire dependence on its wavelength due to the optical Magnus effect. In particular, the resulting frequency increases as the wavelength increases equally for right-handed and left-handed circular polarizations.

B. Black hole shadow

When a general orbit of light is considered, $E \equiv vk$ is conserved. On the other hand, $L_i \equiv \varepsilon^{ijk}x^j k_k$ is not conserved in the presence of optical Magnus effect [40],

$$\frac{dL_i}{dt} = \lambda \left(\frac{x^i}{r} - \frac{k_i x^j k_j}{rk} \right) \partial_r v, \quad (33)$$

but $L^2 = r^2 k^2 - (x^i k_i)^2 = r^2 k^2 \sin^2 \theta$ is conserved. Therefore, $b \equiv cL/E$ is a constant of motion, providing the impact parameter at $r \rightarrow \infty$. The radial equation of motion can be expressed in terms of b as

$$\left(\frac{1}{v} \frac{dr}{dt} \right)^2 = 1 - \left(\frac{bv}{cr} \right)^2, \quad (34)$$

where the right-hand side reaches its minimum at the radius of photon sphere in Eq. (30). When the minimum is positive (negative), the orbit of light can (cannot) cross the photon sphere, corresponding to a plunging (scattering) orbit. The critical impact parameter separating the plunging and scattering orbits then reads

$$b = \frac{cr}{v} \Big|_{\text{Eq.(30)}} = \frac{3\sqrt{3}}{2} r_s. \quad (35)$$

This is the radius of black hole shadow [11], which is again found unaffected by the optical Magnus effect.

Because the anomalous velocity does not contribute to Eq. (34), the radial motion is entirely unaffected by the optical Magnus effect. However, the trajectory of light is indeed affected in the three-dimensional space. As a demonstration, three trajectories obtained by numerical integration of Eq. (28) are shown in Fig. 1 for different wavelengths but with the same impact parameter $b = 2.6r_s$ slightly above the critical value. Although the trajectory of light is restricted to a plane in the geometrical-optics approximation, it deviates toward transverse directions opposite for right-handed and left-handed circular polarizations due to the optical Magnus effect. In particular, the resulting deviation increases as the wavelength increases within the validity range of $k^{-1} \ll r_s$.

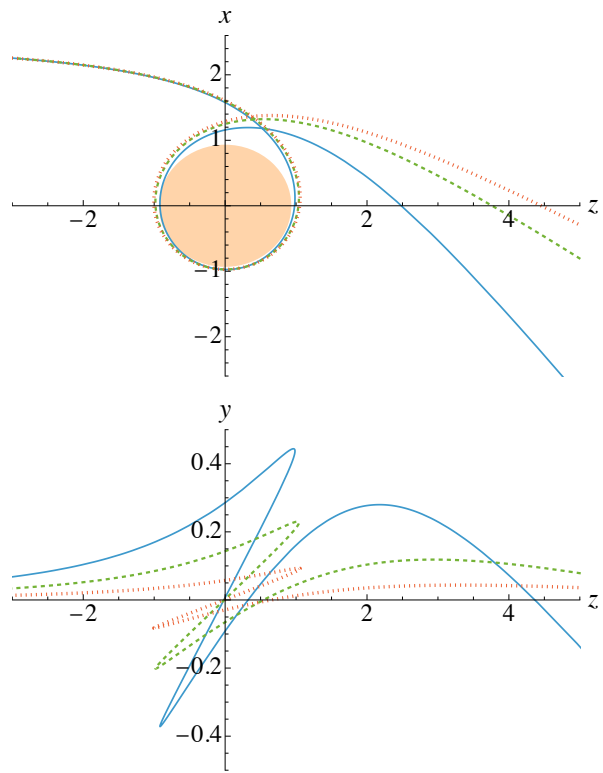


FIG. 1. Trajectories of circularly polarized light with $\lambda = +1$ incident from $\mathbf{x} \rightarrow (2.6, 0, -\infty)$ in units of $r_s = 1$, represented by x (upper panel) and y (lower panel) coordinates as functions of z . The solid (blue), dashed (green), and dotted (red) curves correspond to initial wavevectors of $\mathbf{k} = (0, 0, 1)$, $(0, 0, 2)$, and $(0, 0, 5)$, respectively. The photon sphere (orange) is also presented in the upper panel. The corresponding trajectories for $\lambda = -1$ are obtained by the replacement of $y \rightarrow -y$.

IV. WEAK GRAVITATIONAL POTENTIAL

We then apply the equation of motion for a wave packet of circularly polarized light to the gravitational lensing under a weak gravitational potential $\phi = \phi(\mathbf{x}) \ll c^2$ in an expanding spacetime. The metric is provided by

$$ds^2 = a(t)^2 \left[-(c^2 + 2\phi)dt^2 + \left(1 - \frac{2\phi}{c^2} \right) \delta_{ij} dx^i dx^j \right], \quad (36)$$

so that the equation of motion is brought into

$$\frac{dk_i}{dt} = -\frac{2k}{c} \partial_i \phi, \quad (37a)$$

$$\frac{dx^i}{dt} = v \frac{k_i}{k} - \frac{2\lambda}{c} \varepsilon^{ijk} \partial_j \phi \frac{k_k}{k^2}, \quad (37b)$$

with $v = c + 2\phi/c$. In this section, we work up to the linear order in ϕ and neglect $O(\phi^2)$ without further notes.

A. Deflection and transverse shift

The above equation of motion can be solved perturbatively. We consider a trajectory of light in the form of

$$\mathbf{x} = (b, 0, ct) + O(\phi), \quad (38)$$

$$\mathbf{k} = \frac{k}{c} \frac{d\mathbf{x}}{dt} + O(\phi) = (0, 0, k) + O(\phi), \quad (39)$$

where b is the impact parameter. By changing the parameter from t to $z = x^3$ with $dz/dt = c + O(\phi)$, Eq. (37) for $m = 1, 2$ can be expressed as

$$\frac{dk_m}{dz} = -\frac{2k}{c^2} \partial_m \phi, \quad (40a)$$

$$\frac{dx^m}{dz} = \frac{k_m}{k} - \frac{2\lambda}{c^2 k} \varepsilon^{mn} \partial_n \phi, \quad (40b)$$

with $\varepsilon^{mn} \equiv \varepsilon^{mn3}$. Then, the integration over z under $k_m|_{z \rightarrow -\infty} = 0$ leads to

$$k_m = -\frac{2k}{c^2} \int_{-\infty}^z dz' \partial_m \phi \quad (41)$$

and thus

$$[x^m]_{-\infty}^z = -\frac{2}{c^2} \int_{-\infty}^z dz' (z - z') \partial_m \phi - \frac{2\lambda}{c^2 k} \int_{-\infty}^z dz' \varepsilon^{mn} \partial_n \phi, \quad (42)$$

where ϕ in the integrands is evaluated at $\mathbf{x} = (b, 0, z')$ and $\int_{-\infty}^z dz'' \int_{-\infty}^{z''} dz' = \int_{-\infty}^z dz' \int_{z'}^z dz''$ is employed to perform the integration over z'' . The first term provides the usual deflection of light by the gravitational lensing, whereas the second term is to provide the transverse shift due to the optical Magnus effect.

When the gravitational potential is spherically symmetric, the first and second terms in Eq. (42) contribute only to $x = x^1$ and $y = x^2$, respectively, because of $\partial_m \phi = \delta_{m1}(b/r) \partial_r \phi$. For example, the integration over z' can be performed analytically for $\phi = -GM/r$, so that the trajectory of light reads

$$x = b - r_s \frac{\sqrt{b^2 + z^2} + z}{b}, \quad (43)$$

$$y = \frac{\lambda r_s}{kb} \frac{\sqrt{b^2 + z^2} + z}{\sqrt{b^2 + z^2}}, \quad (44)$$

with $r_s = 2GM/c^2$. Therefore, the deflection angle is found to be

$$\alpha = \left[\frac{dx}{dz} \right]_{-\infty}^{+\infty} = -\frac{2r_s}{b}, \quad (45)$$

whereas the transverse shift to be

$$\Delta y = [y]_{-\infty}^{+\infty} = \frac{2\lambda r_s}{kb}. \quad (46)$$

In particular, the resulting transverse shift is opposite for right-handed and left-handed circular polarizations and increases in magnitude as the wavelength increases within the validity range of $k^{-1}, r_s \ll b$.

B. Lens equation

We now formulate the lens equation incorporating the transverse shift due to the optical Magnus effect. We set the origin at an observer and direct the z axis toward a source located on a plane at $z = z_s > 0$. By considering a reverse trajectory of light from the observer to the source in the form of $\mathbf{x} = (0, 0, ct) + O(\phi)$ and $\mathbf{k} = (0, 0, k) + O(\phi)$, the integration of Eq. (40) over z under $x^m|_{z=0} = 0$ leads to

$$x^m(z_s) = z_s \frac{k_m}{k} \Big|_{z=0} - \frac{2}{c^2} \int_0^{z_s} dz (z_s - z) \partial_m \phi - \frac{2\lambda}{c^2 k} \int_0^{z_s} dz \varepsilon^{mn} \partial_n \phi, \quad (47)$$

where ϕ in the integrands is evaluated at $\mathbf{x} = (x^1(z), x^2(z), z)$. Then, by introducing two-dimensional angular coordinates on the celestial sphere as $\theta_m(z) \equiv (-1)^m x^m(z)/z$, we obtain

$$\theta_m(z_s) = \theta_m(0) - \frac{2}{c^2} \int_0^{z_s} dz \frac{z_s - z}{z_s z} \partial_{\theta_m} \phi - \frac{2\lambda}{c^2 k} \varepsilon^{mn} \partial_n \phi \Big|_{z=0} + \frac{2\lambda}{c^2 k} \int_0^{z_s} dz \frac{1}{z_s z} \varepsilon^{mn} \partial_{\theta_n} \phi. \quad (48)$$

The first line constitutes the usual lens equation for the gravitational lensing [12], which is found to be modified by the optical Magnus effect with the additional second line.

The resulting lens equation is a nonlinear integral equation for $\theta_m(z)$, which can be made tractable in the thin-lens approximation. Namely, by assuming that the gravitational potential produced by a mass density $\rho(\mathbf{x})$ is thin compared to its distances to observer and source, we regard it as localized on a lens plane at $z = z_l \in (0, z_s)$,

$$\phi(\mathbf{x}) \approx \delta(z - z_l) \int dz \phi(\mathbf{x}) = \delta(z - z_l) 2G a_l z_l^2 \int d\theta' \Sigma(\theta') \ln |\boldsymbol{\theta} - \boldsymbol{\theta}'|, \quad (49)$$

where a_l is the scale factor at $z = z_l$ and $\Sigma(\boldsymbol{\theta}) = a_l \int dz \rho(z_l \theta_1, z_l \theta_2, z)$ is the surface mass density projected onto the lens plane. This assumption substituted into Eq. (48) leads to

$$\beta_m = \theta_m - \partial_{\theta_m} \psi(\boldsymbol{\theta}) + \frac{\lambda}{k_s D_{sl}} \varepsilon^{mn} \partial_{\theta_n} \psi(\boldsymbol{\theta}), \quad (50)$$

with the lensing potential provided by

$$\psi(\boldsymbol{\theta}) = \frac{4G}{c^2} \frac{D_{sl} D_l}{D_s} \int d\theta' \Sigma(\theta') \ln |\boldsymbol{\theta} - \boldsymbol{\theta}'|. \quad (51)$$

Here, $\boldsymbol{\beta} \equiv \boldsymbol{\theta}(z_s)$ and $\boldsymbol{\theta} \equiv \boldsymbol{\theta}(0) = \boldsymbol{\theta}(z_l)$ are angular coordinates of source and image, respectively, $D_l = a_l z_l$,

$D_s = a_s z_s$, and $D_{sl} = a_s(z_s - z_l)$ are angular diameter distances from observer to lens, from observer to source, and from lens to source, respectively, and a_s and $k_s = k/a_s$ are the scale factor and the physical wavenumber at $z = z_s$, respectively. Therefore, the gravitational lensing and the optical Magnus effect contribute to the lens equation as longitudinal and transverse derivatives of the lensing potential, respectively, whereas the latter is multiplied by the factor of $\Lambda \equiv \lambda/(k_s D_{sl})$. Its validity range reads $k_s^{-1} \ll l \ll D_l, D_{sl}$ with l being a thickness of lens.

C. Axially symmetric thin lens

1. Generalities

Possible consequences of the optical Magnus effect can be studied in more detail when the lensing potential is axially symmetric under $\Sigma(\boldsymbol{\theta}) = \Sigma(\theta)$. By introducing the mean convergence,

$$\bar{\kappa}(\theta) \equiv \frac{\psi'(\theta)}{\theta} = \frac{4G}{c^2} \frac{D_{sl} D_l}{D_s} \frac{1}{\theta^2} \int_0^\theta d\theta' 2\pi\theta' \Sigma(\theta'), \quad (52)$$

the modified lens equation in the thin-lens approximation is brought into

$$\begin{pmatrix} \beta_1 \\ \beta_2 \end{pmatrix} = \begin{pmatrix} 1 - \bar{\kappa}(\theta) & \Lambda \bar{\kappa}(\theta) \\ -\Lambda \bar{\kappa}(\theta) & 1 - \bar{\kappa}(\theta) \end{pmatrix} \begin{pmatrix} \theta_1 \\ \theta_2 \end{pmatrix}, \quad (53)$$

which relates the magnitudes of $\boldsymbol{\beta}$ and $\boldsymbol{\theta}$ by

$$\beta^2 = ([1 - \bar{\kappa}(\theta)]^2 + [\Lambda \bar{\kappa}(\theta)]^2) \theta^2. \quad (54)$$

Each solution for θ in terms of β predicts an image of a given source formed at

$$\begin{pmatrix} \theta_1 \\ \theta_2 \end{pmatrix} = \left(\frac{\theta}{\beta} \right)^2 \begin{pmatrix} 1 - \bar{\kappa}(\theta) & -\Lambda \bar{\kappa}(\theta) \\ \Lambda \bar{\kappa}(\theta) & 1 - \bar{\kappa}(\theta) \end{pmatrix} \begin{pmatrix} \beta_1 \\ \beta_2 \end{pmatrix}. \quad (55)$$

In particular, $\beta = 0$ corresponds to the exact alignment of source, lens center, and observer on a single line, where the image can appear as an Einstein ring at $\theta = \theta_E > 0$ satisfying $\bar{\kappa}(\theta_E) = 1$ in the absence of optical Magnus effect. However, when the optical Magnus effect is incorporated, Eq. (54) no longer allows solutions at $\theta > 0$ for $\beta = 0$. Therefore, the Einstein ring is found impossible to emerge, being one of the most significant consequences of the optical Magnus effect.

The expansion κ , twist ω , and shear γ_m of image are provided by the Jacobian matrix of the lens equation [12]. From

$$\frac{\partial \beta_m}{\partial \theta_n} = \begin{pmatrix} 1 - \kappa - \gamma_1 & -\gamma_2 - \omega \\ -\gamma_2 + \omega & 1 - \kappa + \gamma_1 \end{pmatrix}_{mn}, \quad (56)$$

we obtain

$$\kappa(\theta) = \bar{\kappa}(\theta) + \frac{\theta}{2} \bar{\kappa}'(\theta), \quad \omega(\theta) = -\Lambda \kappa(\theta), \quad (57)$$

$$\gamma_1(\boldsymbol{\theta}) = \left(\frac{\theta_1^2 - \theta_2^2}{\theta^2} - \Lambda \frac{2\theta_1\theta_2}{\theta^2} \right) \frac{\theta}{2} \bar{\kappa}'(\theta), \quad (58)$$

$$\gamma_2(\boldsymbol{\theta}) = \left(\frac{2\theta_1\theta_2}{\theta^2} + \Lambda \frac{\theta_1^2 - \theta_2^2}{\theta^2} \right) \frac{\theta}{2} \bar{\kappa}'(\theta). \quad (59)$$

The inverse of its determinant also leads to the magnification factor expressed as

$$\mu(\theta) = \frac{1}{[1 - \kappa(\theta)]^2 + [\Lambda \kappa(\theta)]^2 - (1 + \Lambda^2)[\kappa(\theta) - \bar{\kappa}(\theta)]^2}. \quad (60)$$

Therefore, the optical Magnus effect is found to affect the twist, shear, and magnification of image. In particular, its twist is produced solely by the optical Magnus effect and increases in magnitude as the wavelength of light increases within the validity range.

We note that when the magnification factor is divergent at $\theta = \theta_c$, the circle with radius θ_c in the image plane and the corresponding circle with radius $\beta_c = \beta(\theta_c)$ in the source plane are referred to as a critical curve and a caustic, respectively. Because the magnification factor can be expressed in terms of β^2 in Eq. (54) as

$$\mu(\theta) = \left(\frac{d\beta^2}{d\theta^2} \right)^{-1}, \quad (61)$$

θ_c and β_c are provided by an extremum point and the corresponding extremum value of $\beta(\theta)$, respectively. Therefore, when a source crosses the caustic, a pair of images appears or disappears on the critical curve. In particular, we obtain $\theta_c = \theta_E + O(\Lambda^2)$ and $\beta_c = |\Lambda|\theta_E + O(\Lambda^2)$ for $|\Lambda| \ll 1$, where θ_E is the Einstein radius satisfying $\bar{\kappa}(\theta_E) = 1$.

In order to illuminate how image formation is affected by the optical Magnus effect, we consider $\theta = \theta_E + \delta\theta$ with $|\delta\theta| \sim \beta \sim |\Lambda| \ll 1$, so that Eq. (54) is solved by

$$\theta = \theta_E \pm \frac{\sqrt{\beta^2 - \Lambda^2 \theta_E^2}}{\theta_E \bar{\kappa}'(\theta_E)} + O(\Lambda^2). \quad (62)$$

Whereas such two solutions exist for $\beta > |\Lambda|\theta_E$, they merge at $\theta = \theta_E$ for $\beta = |\Lambda|\theta_E$ and then disappear for $\beta < |\Lambda|\theta_E$. The angular coordinates where the pair of images merges are obtained from Eq. (55),

$$\begin{pmatrix} \theta_1 \\ \theta_2 \end{pmatrix}_{\beta=|\Lambda|\theta_E} = \frac{\theta_E}{|\Lambda|} \begin{pmatrix} 0 & -\Lambda \\ \Lambda & 0 \end{pmatrix} \begin{pmatrix} \hat{\beta}_1 \\ \hat{\beta}_2 \end{pmatrix} + O(\Lambda), \quad (63)$$

which is a point on the Einstein radius but rotated by ± 90 degrees from the direction of source in the limit of $|\Lambda| \ll 1$. In particular, the resulting rotation of image is opposite for right-handed and left-handed circular polarizations of light. This is another significant consequence of the optical Magnus effect, which is to be demonstrated with simple lens models.

2. Simple lens models

Apart from the general discussion, the modified lens equation in the thin-lens approximation can be solved analytically for a point mass lens with $\rho = (M/a_l^3)\delta(\mathbf{x})$. The mean convergence reads

$$\bar{\kappa}(\theta) = \left(\frac{\theta_E}{\theta}\right)^2, \quad \theta_E^2 = \frac{4GM}{c^2} \frac{D_{sl}}{D_s D_l}, \quad (64)$$

so that Eq. (54) is solved by $\theta = \theta_{\pm}$ with

$$\theta_{\pm}^2 = \frac{\beta^2}{2} + \theta_E^2 \pm \sqrt{\left(\frac{\beta^2}{2} + \theta_E^2\right)^2 - (1 + \Lambda^2)\theta_E^4}. \quad (65)$$

Whereas such two solutions exist for $\beta^2 > \beta_0^2 \equiv 2(\sqrt{1 + \Lambda^2} - 1)\theta_E^2$, they merge at $\theta^2 = \theta_0^2 \equiv \sqrt{1 + \Lambda^2}\theta_E^2$ for $\beta = \beta_0$ and then disappear for $\beta < \beta_0$. Because the magnification factor is provided by

$$\mu(\theta) = \frac{\theta^4}{\theta^4 - (1 + \Lambda^2)\theta_E^4}, \quad (66)$$

the radii of critical curve and caustic are found to be $\theta_c = \theta_0$ and $\beta_c = \beta_0$, respectively, for the point mass lens.

Similarly, the same equation can be solved analytically for a singular isothermal sphere with $\rho = \sigma_v^2/(2\pi G a_l^2 r^2)$. The mean convergence reads

$$\bar{\kappa}(\theta) = \frac{\theta_E}{\theta}, \quad \theta_E = \frac{4\pi\sigma_v^2}{c^2} \frac{D_{sl}}{D_s}, \quad (67)$$

so that Eq. (54) is solved by $\theta = \theta_{\pm}$ with

$$\theta_{\pm} = \theta_E \pm \sqrt{\beta^2 - \Lambda^2\theta_E^2}. \quad (68)$$

Whereas only the upper solution exists for $\beta > \sqrt{1 + \Lambda^2}\theta_E$, the lower solution appears at $\theta = 0$ for $\beta = \sqrt{1 + \Lambda^2}\theta_E$. Therefore, the two solutions exist for $|\Lambda|\theta_E < \beta \leq \sqrt{1 + \Lambda^2}\theta_E$, but they merge at $\theta = \theta_E$ for $\beta = |\Lambda|\theta_E$ and then disappear for $\beta < |\Lambda|\theta_E$. Because the magnification factor is provided by

$$\mu(\theta) = \frac{\theta}{\theta - \theta_E}, \quad (69)$$

the radii of critical curve and caustic are found to be $\theta_c = \theta_E$ and $\beta_c = |\Lambda|\theta_E$, respectively, for the singular isothermal sphere.

The angular coordinates of each image are obtained by substituting $\theta = \theta_{\pm}$ into Eq. (55), which are shown in Fig. 2 separately for the point mass lens and for the singular isothermal sphere. Although a pair of images outside and inside the critical curve appears in parallel to a source in the geometrical-optics approximation, their locations deviate toward transverse directions opposite for right-handed and left-handed circular polarizations due to the optical Magnus effect. In particular, the resulting deviation is significant even for an infinitesimal wavelength of light when the source is located slightly outside the caustic, whereas the source inside forms no images.

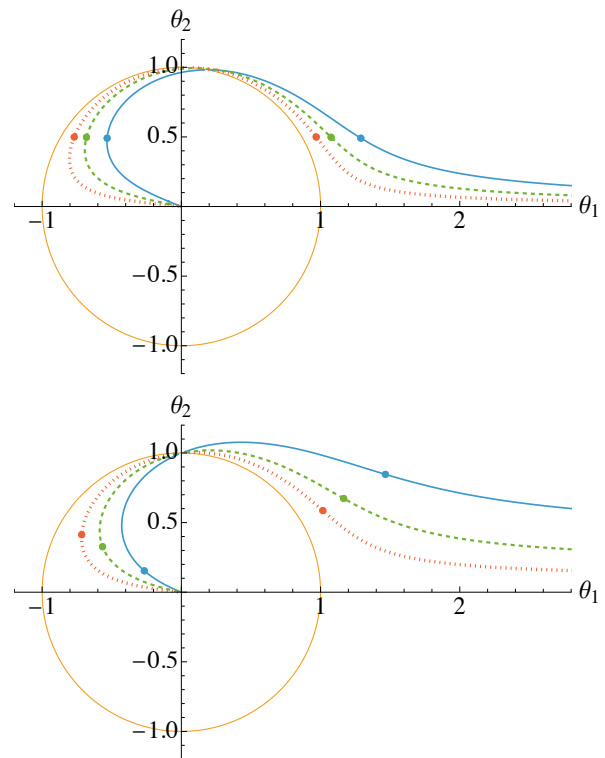


FIG. 2. Angular coordinates of image by circularly polarized light with $\lambda = +1$ for the point mass lens (upper panel) and for the singular isothermal sphere (lower panel) in units of $\theta_c = 1$. The solid (blue), dashed (green), and dotted (red) curves correspond to $|\Lambda| = 0.4, 0.2$, and 0.1 , respectively, for a source located at $\beta = (\beta, 0)$ with β varied over $[\beta_c, \infty)$. A pair of images outside and inside the critical curve (orange) appears for $\beta > \beta_c$ and their locations for $\beta = 2\beta_c$ are presented by dots. They move closer to (away from) the critical curve as β decreases (increases) and merge on the critical curve for $\beta = \beta_c$, whereas no images are formed for $\beta < \beta_c$. The corresponding images for $\lambda = -1$ are obtained by the replacement of $\theta_2 \rightarrow -\theta_2$.

V. SUMMARY

Finally, our findings are summarized as follows. In Sec. II, we derived the equation of motion for a wave packet of circularly polarized light starting from Maxwell's equations in a curved spacetime. Although the known result involving the helicity-dependent anomalous velocity is confirmed, our alternative derivation allows an expanding spacetime as well as a strong gravitational potential.

In Sec. III, we applied the resulting equation of motion to the gravitational lensing in the Schwarzschild spacetime. Although the radii of photon sphere and black hole shadow are unaffected by the optical Magnus effect, the frequency of circular motion of light is found to increase as the wavelength increases. We also demonstrated that a general orbit of light is no longer restricted to a plane but deviates toward transverse directions opposite for right-

handed and left-handed circular polarizations due to the optical Magnus effect.

In Sec. IV, we studied the gravitational lensing under a weak gravitational potential in an expanding spacetime. By formulating the lens equation modified to incorporate the optical Magnus effect, the Einstein ring is found impossible to emerge from a point source for any axially symmetric thin lens. This is because the optical Magnus effect makes a caustic acquire nonzero radius so that a source inside no longer forms images near the Einstein radius. When the source is located outside, a pair of images appears and their locations can deviate significantly toward transverse directions even for an infinitesimal wavelength of light.

Possible consequences of the optical Magnus effect on gravitational lensing are thus illuminated as a matter of principle. Since they are typically suppressed by a factor of the wavelength of light over astrophysical length scales, future work should be devoted to finding observable signatures sensitive to the optical Magnus effect. It is also worthwhile to extend our derivation of the equation of motion to an arbitrary spacetime metric for a wave packet of circularly polarized light as well as gravitational wave, which may provide us with insights complementary to previous approaches [29–32].

ACKNOWLEDGMENTS

The author thanks Teruaki Suyama for valuable discussion. This work was supported by JSPS KAKENHI Grant No. JP21K03384 and Matsuo Foundation.

Appendix A: Geodesic equation

The geodesic equation is provided by

$$\frac{dk^a}{ds} + \Gamma^a_{bc} k^b k^c = 0, \quad (\text{A1})$$

or equivalently,

$$\frac{dk_a}{ds} - \frac{1}{2} \partial_a g_{bc} k^b k^c = 0, \quad (\text{A2})$$

where s is the affine parameter and $k^a = dx^a/ds$ is the wavevector satisfying $g_{ab} k^a k^b = 0$ for light. Under the background spacetime in Eq. (13), the null condition leads to

$$(k^0)^2 = \frac{C(\mathbf{x})}{A(\mathbf{x})} (k^j)^2 = \frac{(k_j)^2}{a(t)^4 A(\mathbf{x}) C(\mathbf{x})}, \quad (\text{A3})$$

whereas the geodesic equation for $i = 1, 2, 3$ reads

$$\begin{aligned} \frac{dk_i}{ds} &= -\frac{1}{2} a(t)^2 \partial_i A(\mathbf{x}) (k^0)^2 + \frac{1}{2} a(t)^2 \partial_i C(\mathbf{x}) (k^j)^2 \\ &= -\frac{(k_j)^2}{2a(t)^2 A(\mathbf{x})} \partial_i \left[\frac{A(\mathbf{x})}{C(\mathbf{x})} \right]. \end{aligned} \quad (\text{A4})$$

By changing the parameter from s to $t = x^0$ with $dt/ds = k^0$, we obtain

$$\frac{dk_i}{dt} = \frac{ds}{dt} \frac{dk_i}{ds} = -|\mathbf{k}| \partial_i v(\mathbf{x}), \quad (\text{A5})$$

which is equivalent to Eq. (25) under $v(\mathbf{x}) = \sqrt{A(\mathbf{x})/C(\mathbf{x})}$ and $|\mathbf{k}| = \sqrt{(k_j)^2}$. Similarly, by employing $k^i = dx^i/ds$, we also obtain

$$\frac{dx^i}{dt} = \frac{ds}{dt} \frac{dx^i}{ds} = v(\mathbf{x}) \frac{k_i}{|\mathbf{k}|}, \quad (\text{A6})$$

which is equivalent to the first term of Eq. (26).

Appendix B: Gravitational wave

Einstein's equations linearized with respect to an expanding flat spacetime $ds^2 = a^2(-dt^2 + \delta_{ij} dx^i dx^j)$ are provided by

$$\partial_t^2 h_{ij} + \frac{2\dot{a}}{a} \partial_t h_{ij} - \partial_k \partial_k h_{ij} = 0, \quad (\text{B1})$$

where $h_{ij} \ll 1$ is a tensor perturbation in transverse-traceless gauge satisfying $\partial_i h_{ij} = h_{ii} = 0$ [41]. We then introduce gravito-electric and gravito-magnetic fields as

$$E_{ij} = -a \partial_t h_{ij}, \quad B_{ij} = a \varepsilon^{ikl} \partial_k h_{lj}, \quad (\text{B2})$$

which are also symmetric, transverse, and traceless [42]. Because of $\varepsilon^{ikl} \partial_k B_{lj} = -a \partial_k \partial_k h_{ij}$, we obtain

$$\partial_t E_{ij} = -\frac{\dot{a}}{a} E_{ij} + \varepsilon^{ikl} \partial_k B_{lj}, \quad (\text{B3})$$

$$\partial_t B_{ij} = +\frac{\dot{a}}{a} B_{ij} - \varepsilon^{ikl} \partial_k E_{lj}, \quad (\text{B4})$$

and such a pair of equations can be combined into

$$\partial_t \Psi_{ij} = -\frac{\dot{a}}{a} \Psi_{ij}^* - i \varepsilon^{ikl} \partial_k \Psi_{lj}, \quad (\text{B5})$$

with $\Psi_{ij} \equiv (E_{ij} + iB_{ij})/\sqrt{2}$. Because the first term does not allow the energy conservation, we assume $\dot{a} = 0$ from now on, leading to the continuity equation in the usual form of $\partial_t (\Psi_{ij}^* \Psi_{ij}) + \partial_k (-i \varepsilon^{kil} \Psi_{ij}^* \Psi_{lj}) = 0$.

The equation of motion for a wave packet of gravitational wave can be derived in parallel to Sec. II B. One important difference is that the Fourier representation of complex gravito-electromagnetic field reads

$$\Psi_{ij}(t, \mathbf{x}) = \int \frac{d\mathbf{k}}{(2\pi)^3} \psi(t, \mathbf{k}) e_{ij}(\mathbf{k}) e^{\lambda i \mathbf{k} \cdot \mathbf{x}}. \quad (\text{B6})$$

Here, $e_{ij}(\mathbf{k}) \equiv e_i(\mathbf{k}) e_j(\mathbf{k})$ is defined in terms of the complex polarization vector in Eq. (16), so that $\Psi_{ij}(t, \mathbf{x})$ is symmetric, transverse, and traceless, and $\lambda = \pm 1$ specifies the sign of helicity corresponding to right-handed and

left-handed circular polarizations. It is then straightforward to obtain the Lagrangian,

$$L = \bar{k}_i(t)\dot{\bar{x}}^i(t) - c|\bar{\mathbf{k}}(t)| - \dot{\bar{k}}_i(t)\mathcal{A}^i(\bar{\mathbf{k}}(t)), \quad (\text{B7})$$

where c is presented explicitly and the Berry connection is provided by $\mathcal{A}^i(\mathbf{k}) = -\lambda i e_{jk}^*(\mathbf{k})\partial_{k_i} e_{jk}(\mathbf{k})$.

We now consider a curved spacetime described by Eq. (13) with $a(t) = 1$. Possible corrections to the above Lagrangian include replacing c by $v(\mathbf{x}) = \sqrt{A(\mathbf{x})/C(\mathbf{x})}$ as well as adding terms involving its derivatives. Under such replacement, the Euler-Lagrange equations with re-

spect to $\bar{x}^i(t)$ and $\bar{k}_i(t)$ lead to Eqs. (25) and (26), respectively, but with λ replaced by 2λ because the Berry curvature is provided by $\mathcal{B}(\mathbf{k}) = 2\lambda\mathbf{k}/|\mathbf{k}|^3$. Therefore, the optical Magnus effect with twice the anomalous velocity is expected for gravitational waves with circular polarizations, which should be referred to as the *gravitational Magnus effect*. In particular, all the consequences discussed in Secs. III and IV are applicable by regarding $\lambda \rightarrow \pm 2$ as the helicity of circularly polarized gravitational wave. However, our heuristic derivation of the equation of motion does not exclude other additional corrections at the linear order in wavelength.

-
- [1] U. Seljak, “Measuring polarization in the cosmic microwave background,” *Astrophys. J.* **482**, 6-16 (1997).
- [2] U. Seljak and M. Zaldarriaga, “Signature of gravity waves in the polarization of the microwave background,” *Phys. Rev. Lett.* **78**, 2054-2057 (1997).
- [3] M. Kamionkowski, A. Kosowsky, and A. Stebbins, “A Probe of primordial gravity waves and vorticity,” *Phys. Rev. Lett.* **78**, 2058-2061 (1997).
- [4] M. Kamionkowski and E. D. Kovetz, “The Quest for B modes from inflationary gravitational waves,” *Annu. Rev. Astron. Astrophys.* **54**, 227-269 (2016).
- [5] K. Akiyama *et al.* (Event Horizon Telescope Collaboration), “First M87 Event Horizon Telescope results. VII. Polarization of the ring,” *Astrophys. J. Lett.* **910**, L12 (2021).
- [6] K. Akiyama *et al.* (Event Horizon Telescope Collaboration), “First M87 Event Horizon Telescope results. VIII. Magnetic field structure near the event horizon,” *Astrophys. J. Lett.* **910**, L13 (2021).
- [7] I. Lioudakis *et al.*, “Polarized blazar X-rays imply particle acceleration in shocks,” *Nature (London)* **611**, 677-681 (2022).
- [8] D. M. Eardley, D. L. Lee, A. P. Lightman, R. V. Wagoner, and C. M. Will, “Gravitational-wave observations as a tool for testing relativistic gravity,” *Phys. Rev. Lett.* **30**, 884-886 (1973).
- [9] D. M. Eardley, D. L. Lee, and A. P. Lightman, “Gravitational-wave observations as a tool for testing relativistic gravity,” *Phys. Rev. D* **8**, 3308-3321 (1973).
- [10] C. M. Will, “The confrontation between general relativity and experiment,” *Living Rev. Relativity* **17**, 4 (2014).
- [11] C. W. Misner, K. S. Thorne, and J. A. Wheeler, *Gravitation* (Freeman, San Francisco, 1973).
- [12] P. Schneider, J. Ehlers, and E. E. Falco, *Gravitational Lenses* (Springer-Verlag, Berlin Heidelberg, 1992).
- [13] A. V. Dooghin, N. D. Kundikova, V. S. Liberman, and B. Ya. Zel’dovich, “Optical Magnus effect,” *Phys. Rev. A* **45**, 8204-8208 (1992).
- [14] V. S. Liberman and B. Ya. Zel’dovich, “Spin-orbit interaction of a photon in an inhomogeneous medium,” *Phys. Rev. A* **46**, 5199-5207 (1992).
- [15] K. Yu. Bliokh and Yu. P. Bliokh, “Topological spin transport of photons: the optical Magnus effect and Berry phase,” *Phys. Lett. A* **333**, 181-186 (2004).
- [16] K. Yu. Bliokh and Yu. P. Bliokh, “Modified geometrical optics of a smoothly inhomogeneous isotropic medium: The anisotropy, Berry phase, and the optical Magnus effect,” *Phys. Rev. E* **70**, 026605 (2004).
- [17] M. Onoda, S. Murakami, and N. Nagaosa, “Hall effect of light,” *Phys. Rev. Lett.* **93**, 083901 (2004).
- [18] K. Y. Bliokh, F. J. Rodríguez-Fortuño, F. Nori, and A. V. Zayats, “Spin-orbit interactions of light,” *Nature Photon.* **9**, 796-808 (2015).
- [19] X. Ling, X. Zhou, K. Huang, Y. Liu, C.-W. Qiu, H. Luo, and S. Wen, “Recent advances in the spin Hall effect of light,” *Rep. Prog. Phys.* **80**, 066401 (2017).
- [20] F. de Felice, “On the gravitational field acting as an optical medium,” *Gen. Relat. Gravit.* **2**, 347-357 (1971).
- [21] A. Bérard and H. Mohrbach, “Spin Hall effect and Berry phase of spinning particles,” *Phys. Lett. A* **352**, 190-195 (2006).
- [22] P. Gosselin, A. Bérard, and H. Mohrbach, “Spin Hall effect of photons in a static gravitational field,” *Phys. Rev. D* **75**, 084035 (2007).
- [23] V. P. Frolov and A. A. Shoom, “Spinoptics in a stationary spacetime,” *Phys. Rev. D* **84**, 044026 (2011).
- [24] C.-M. Yoo, “Notes on spinoptics in a stationary spacetime,” *Phys. Rev. D* **86**, 084005 (2012).
- [25] N. Yamamoto, “Photonic chiral vortical effect,” *Phys. Rev. D* **96**, 051902(R) (2017).
- [26] N. Yamamoto, “Spin Hall effect of gravitational waves,” *Phys. Rev. D* **98**, 061701(R) (2018).
- [27] C. Duval and T. Schücker, “Gravitational birefringence of light in Robertson-Walker cosmologies,” *Phys. Rev. D* **96**, 043517 (2017).
- [28] C. Duval, L. Marsot, and T. Schücker, “Gravitational birefringence of light in Schwarzschild spacetime,” *Phys. Rev. D* **99**, 124037 (2019).
- [29] M. A. Oancea, J. Joudioux, I. Y. Dodin, D. E. Ruiz, C. F. Paganini, and L. Andersson, “Gravitational spin Hall effect of light,” *Phys. Rev. D* **102**, 024075 (2020).
- [30] V. P. Frolov, “Maxwell equations in a curved spacetime: Spin optics approximation,” *Phys. Rev. D* **102**, 084013 (2020).
- [31] L. Andersson, J. Joudioux, M. A. Oancea, and A. Raj, “Propagation of polarized gravitational waves,” *Phys. Rev. D* **103**, 044053 (2021).
- [32] A. I. Harte and M. A. Oancea, “Spin Hall effects and the localization of massless spinning particles,” *Phys. Rev. D* **105**, 104061 (2022).
- [33] M. A. Oancea, C. F. Paganini, J. Joudioux, and L. Andersson, “An overview of the gravitational spin Hall ef-

- fect,” arXiv:1904.09963 [gr-qc].
- [34] L. Andersson and M. A. Oancea, “Spin Hall effects in the sky,” *Class. Quantum Grav.* **40**, 154002 (2023).
- [35] K. S. Thorne and D. Macdonald, “Electrodynamics in curved spacetime: 3 + 1 formulation,” *Mon. Not. R. Astron. Soc.* **198**, 339-343 (1982).
- [36] M. Alcubierre, J. C. Degollado, and M. Salgado, “Einstein-Maxwell system in 3 + 1 form and initial data for multiple charged black holes,” *Phys. Rev. D* **80**, 104022 (2009).
- [37] T. W. Baumgarte and S. L. Shapiro, *Numerical Relativity: Solving Einstein’s Equations on the Computer* (Cambridge University Press, Cambridge, 2010).
- [38] M.-C. Chang and Q. Niu, “Berry phase, hyperorbits, and the Hofstadter spectrum: Semiclassical dynamics in magnetic Bloch bands,” *Phys. Rev. B* **53**, 7010-7023 (1996).
- [39] G. Sundaram and Q. Niu, “Wave-packet dynamics in slowly perturbed crystals: Gradient corrections and Berry-phase effects,” *Phys. Rev. B* **59**, 14915-14925 (1999).
- [40] We note that $J_i \equiv L_i + \lambda k_i/k$ is conserved, which is reminiscent of the total angular momentum [17].
- [41] M. Maggiore, *Gravitational Waves. Vol. 2: Astrophysics and Cosmology* (Oxford University Press, Oxford, 2018).
- [42] S. M. Barnett, “Maxwellian theory of gravitational waves and their mechanical properties,” *New J. Phys.* **16**, 023027 (2014).